

Dual application of Chebyshev polynomial for efficiently computing thousands of central eigenvalues in many-spin systems

Haoyu Guan and Wenxian Zhang*

School of Physics and Technology, Wuhan University, Wuhan, Hubei 430072, China

(Dated: November 5, 2020)

It is known that the statistical properties of the spectrum provide an essential characterization of quantum chaos. The computation of a large group of interior eigenvalues at the middle spectrum is thus an important problem for quantum many-body systems. We propose a dual application of Chebyshev polynomial (DACP) method to efficiently find thousands of central eigenvalues, which are exponentially close to each other in terms of the system size. To cope with the near-degenerate problem, we use the Chebyshev polynomial to both construct an exponential of semicircle filter as the preconditioning step and generate a large set of proper states as the basis of the desired subspace. Besides, DACP owes an excellent property that its computation time is not influenced by the required number of eigenvalues. Numerical experiments on Ising spin chain and spin glass shards show the correctness and efficiency of the proposed method. As our results demonstrate, DACP is a factor of 30 faster than the state-of-the-art shift-invert method for the Ising spin chain while 8 times faster for the spin glass shards. The memory requirements scale better with system size and could be a factor of 100 less than in the shift-invert approach.

I. INTRODUCTION

It has been realized that the energy level statistics provide an essential characterization of quantum chaos [1, 2]. Indeed, it is generally believed that integrable systems imply the absence of level repulsion and a Poisson distribution of energy level spacings [2], while chaotic systems exhibit strong level repulsion and a Wigner-Dyson distribution [3]. Besides, there are other useful statistical tools like the δ_3 statistic [4] and the power spectrum of the δ_n statistic [5]. The numerical observation of eigenvalues are important to exactly characterize these level statistics. As far as we know, there has been no direct theoretical derivation for the suggested behavior of the level statistics.

In addition, the need to access individual eigenstates in the middle of the spectrum, which corresponds to the “infinite temperature” limit, is emphasized in studying the phenomenon of many-body localization (MBL) [6–8]. Numerical simulations remain instrumental in understanding quantitatively many aspects of the MBL problem. Many methods based on the specific properties of eigenstates in the MBL phase have been proposed [9–11], however, one often requires a numerical method that works in both the MBL and the thermal phase in unbiased manner to probe the full phase diagram.

In this work, we propose a numerical method to efficiently find thousands of eigenvalues/eigenstates in the middle of the energy band, which is already helpful to construct the level statistics [12, 13]. As the many-body problems of interest often involve a huge Hilbert space dimension growing exponentially in terms of system size, it is typically unfeasible to conduct a full diagonalization or to solve the time-independent Schrödinger equation.

Therefore, seeking to resolve the eigenvalue problem in a small part of the spectrum is an unavoidable and desirable substitution.

Many numerical methods, such as quantum Monte Carlo [14, 15], the traditional density matrix renormalization group (DMRG) method [16] and matrix product states (MPS) [17–19] have been developed to solve the ground states of quantum many-body systems. But all of them are insufficient to find those highly excited eigenstates. To access the interior eigenstates, including the central ones, a strategy described as matrix spectroscopy is often invoked [20–22]. It aims at computing eigenstates in selected regions of the spectrum. To this end hybrid techniques that coupling the ground state solvers with a spectral filter have been proposed, where the filter is designed to cast the selected interior regions to the edges of the spectrum. Even if equipped with a spectral filter, there are still severe restrictions for the above methods. The quantum Monte Carlo suffers from the widely known sign problem, which often requires an exponential amount of computational resources to obtain a reasonable accuracy [23, 24]. Besides, it is known that the efficiency of the tensor network approaches are limited to the systems whose ground states must obey the area law; i.e., the von Neuman entropy of the reduced density matrix of a subsystem scales with the subsystem’s area [25, 26].

In many aspects, the Green function $(\mathcal{H} - \lambda I)^{-1}$ is an excellent spectral filter. The result of using it is that the cluster of eigenvalues near the test energy λ are mapped to very large positive and negative values, which generally improves the convergence. The Lanczos method [27] has been coupled with it [20, 21], and the Chebyshev polynomial expansion of the Green function is employed in [28]. In particular, the shift-invert method [29] essentially takes use of this spectral transformation and it has been widely used in quantum many-spin systems [30–33]. Moreover, it was even found to be the most efficient one

* wxzhang@whu.edu.cn

for the MBL problem [8]. However, for large systems this method suffers a rapid scaling of resources due to a factorization of the matrix $(\mathcal{H} - \lambda I)^{-1}$ [8], which may be prohibitively expensive.

Other spectral filters have been also proposed. The Dirac delta function expanded by the Chebyshev polynomial, which is quite similar to the Green function, constitutes another choice. It has been successfully combined with both the Lanczos method and the Davidson method [34–36]. The Chebyshev filter diagonalization method also applies the Chebyshev expansion to the rectangular window function [37]. However, all these methods, including the shift-invert method, are not designed for large scale eigenvalue computations. They share a property that the computation time is roughly proportional to the required number of eigenvalues, i.e., to find more eigenvalues means more filtration.

In this paper, we present a dual application of Chebyshev polynomial (DACP) method to efficiently find a large amount of eigenvalues through fully exploring the excellent properties of the Chebyshev polynomial. We focus on eigenvalues at the middle of the spectrum, which is generally the region of the highest density of states. By employing the Chebyshev polynomial for the first time, we construct the exponential of semicircle (exp-semicircle) filter to efficiently and vastly damp the unwanted part of the spectrum. The second application of the Chebyshev polynomial is to fast search a set of linearly independent states to span the specific subspace that consists of all those eigenstates corresponding to the wanted eigenvalues. The new eigenvalue problem restricted in this small subspace is then easily solved. For real problems in many-spin systems, the DACP method is a very efficient tool. We find that for a large class of many-spin systems, it gives a significant increase in the computation speed, sometimes up to a factor of 30, in comparison with the shift-invert method. Moreover, the memory saving is even more drastic, up to a factor of 100. It is different from the iterative methods mentioned above in that its convergence time is only slightly varied when the required eigenvalue number is vastly changed. Test cases using only a single core are presented, with calculating 5,000 eigenvalues for the Hilbert space dimension up to 5×10^5 , or the system with 19 spins.

The remainder of the manuscript is organized as follows. The required backgrounds and detailed formalism, especially the two different applications of the Chebyshev polynomial, are given in Sec. II. In Sec. III we carry out a numerical trial of the DACP method by calculating eigenvalues for both the Ising model and the spin glass shards. A conclusion is given in Sec. IV.

II. DUAL APPLICATION OF CHEBYSHEV POLYNOMIAL METHOD

To access eigenvalues of large spin systems, we restrict ourselves with a matrix-free mode, i.e., the matrix of

Hamiltonian is not explicitly expressed. Instead, we view the Hamiltonian \mathcal{H} as a function whose input and output are both states/vectors. Therefore, we shall only operate with the quantum states $|\psi\rangle, \mathcal{H}|\psi\rangle, \dots, \mathcal{H}^k|\psi\rangle$, where k is a positive integer with an appropriate value (not too large), in the original Hilbert space of dimension up to 5×10^5 . In this paper, we set to find 5,000 eigenvalues in the middle of the spectrum for many-spin systems.

The basic idea is fairly simple and straightforward. We first transform a randomly initialized state into a wave packet in the energy representation, which lies in the subspace spanned by at least 5,000 central eigenstates. With this particular state in hand, we then generate a large amount of linearly independent states, as large as possible, to approximately span the subspace consisting the required eigenstates. Once the set of linearly independent vectors is known, one may explicitly calculate \mathcal{H}_{sub} , the matrix representation of \mathcal{H} in this subspace. The remained operations are restricted in the space of dimension around 10^4 . Finally, direct diagonalization of \mathcal{H}_{sub} , which is of size $10^4 \times 10^4$, gives the required eigenvalues. The detailed procedures and discussions will be given in the subsections below.

A. Chebyshev Polynomial

Note that only the polynomial combinations of \mathcal{H} are the allowed operations. We utilize the Chebyshev polynomial to fulfill the tasks mentioned above. It is the key idea to bridge the combinations of \mathcal{H}^k with an exponential function of \mathcal{H} , either $\exp(k\mathcal{H})$ or $\exp(ik\mathcal{H})$. Due to its several remarkable properties, we think that the Chebyshev polynomial exhausts the potential of this type of methods.

The k th order Chebyshev polynomial of the first kind is defined by

$$T_k(x) = \begin{cases} \cos(k \cos^{-1}(x)), & |x| \leq 1 \\ \cosh(k \cosh^{-1}(x)), & x > 1 \\ (-1)^k \cosh(k \cosh^{-1}(-x)), & x < -1 \end{cases}, \quad (1)$$

with initial conditions $T_0(x) = 1$ and $T_1(x) = x$ [38]. It is a piece-wise function containing two different kinds of expression. For simplicity, let us set $\theta = \cos^{-1}(x)$ ($\cos \theta = x$) when $x \in [-1, 1]$ and set $\theta = \cosh^{-1}(x)$ when $x \in [1, \infty)$, the corresponding range of θ is $\theta \in [0, \pi]$ and $\theta \in [0, \infty)$, respectively. In terms of the variable θ , Eq. (1) becomes

$$T_k(x) = \begin{cases} \cos(k\theta), & |x| \leq 1 \\ \cosh(k\theta), & x > 1. \end{cases} \quad (2)$$

One may easily observe that $T_k(x)$ is a sine or cosine-like oscillation function bounded by -1 and 1 inside the interval $[-1, 1]$, as illustrated in Fig. 1 (a-c), while it grows extremely fast outside $[-1, 1]$, as shown in Fig. 1 (d-f).

Note that $\cosh(k\theta) = (e^{k\theta} + e^{-k\theta})/2$, it is natural to expect an exponential growth of the Chebyshev polynomial outside the interval $[-1, 1]$. In fact, it is known that

among all polynomials with degree $\leq k$, the Chebyshev polynomial $T_k(x)$ grows the fastest outside the interval $[-1, 1]$ under comparable conditions [39].

Associated with those properties is a practically useful one: $T_{k+1}(x)$ can be efficiently determined by using the 3-term recurrence

$$T_{k+1}(x) = 2xT_k(x) - T_{k-1}(x). \quad (3)$$

All these properties of the Chebyshev polynomial render it a powerful toolbox and are of great use for the DACP method.

B. Exp-semicircle Filter

We utilize the exponential growth of the Chebyshev polynomial outside the interval $[-1, 1]$ to efficiently construct an exp-semicircle filter, as shown in Fig. 2. It drastically amplifies the components of a certain range of eigenstates for any randomly initialized states, resulting to a new state that localized in the central spectrum. We note that the Chebyshev filter explores the same property as well, except that it aims at amplifying the lower end of the spectrum [40, 41]. A similar approach has been also appeared in the quantum algorithm for finding ground states [42].

In detail, for the Hamiltonian \mathcal{H} with a spectrum bounded in $[E_{\min}, E_{\max}]$, where E_{\min} is the minimum energy and E_{\max} the maximum energy, the exp-semicircle filter is designed to amplify the components of the eigenstates corresponding to eigenvalues in the interval $[-a, a]$

and to simultaneously dampen those in the interval $[E_{\min}, -a]$ and $[a, E_{\max}]$, where a is a real positive parameter. Focusing on the spin systems, we have assumed $E_{\min} < -a$ and $a < E_{\max}$. After the filtration, a new state consists of the eigenstates with eigenvalues belong to the interval $[-a, a]$ is generated. For simplicity, let us mark the subspace spanned by the eigenstates contained in $[-a, a]$ as \mathbb{L} .

We now introduce the specific implementation details. Note that we want to amplify the middle of the spectrum, but the exponential growth of the Chebyshev polynomial exists only in both ends. To satisfy this goal, we consider the squared Hamiltonian \mathcal{H}^2 with a spectrum range $[0, E_{\max}^2]$ (suppose $E_{\min} = -E_{\max}$ for simplicity). The central spectrum $[-a, a]$ of \mathcal{H} is transferred to $[0, a^2]$ for \mathcal{H}^2 , which is exactly the lower end of the spectrum of \mathcal{H}^2 . Next is to map the dampening part $[a^2, E_{\max}^2]$ into $[-1, 1]$ by shift and normalization of \mathcal{H}^2 , we thus define a new operator

$$\mathcal{F} = \frac{\mathcal{H}^2 - E_c}{E_0}, \quad (4)$$

where $E_c = (E_{\max}^2 + a^2)/2$ and $E_0 = (E_{\max}^2 - a^2)/2$. One may easily affirm this map's correctness by replacing \mathcal{H}^2 with either a^2 or E_{\max}^2 , and correspondingly we have $F(x) = (x^2 - E_c)/E_0$. Note that \mathcal{F} is simply a polynomial expression of \mathcal{H} , so is $T_k(\mathcal{F})$.

We then explore the effect of the filtration using $T_k(\mathcal{F})$. As the eigenvalues inside $[0, a^2]$ of \mathcal{H}^2 is mapped into $[-1 - 2a^2/(E_{\max}^2 - a^2), -1]$ of \mathcal{F} , we have $T_k(\mathcal{F}) =$

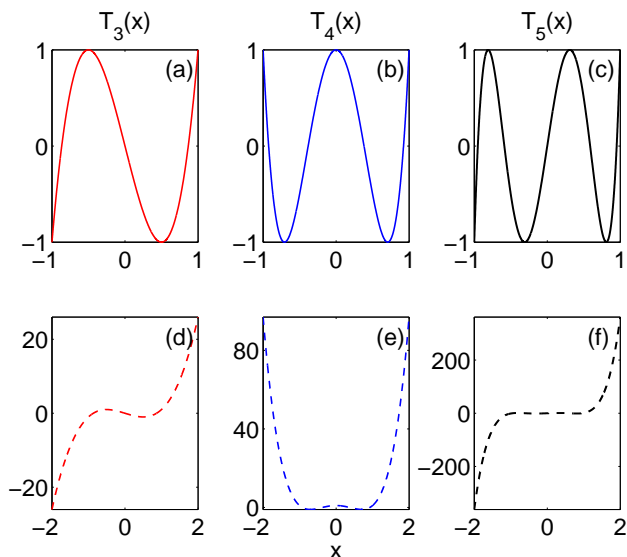


FIG. 1. (Color online.) Chebyshev polynomials $T_k(x)$ for $k = 3$ (red lines), $k = 4$ (blue lines), $k = 5$ (black lines). The first row ((a-c) with solid lines) illustrate the oscillations of $T_k(x)$ inside the interval $[-1, 1]$ while the second row ((d-f) with dashed lines) show the rapid increase outside $[-1, 1]$ of Chebyshev polynomials.

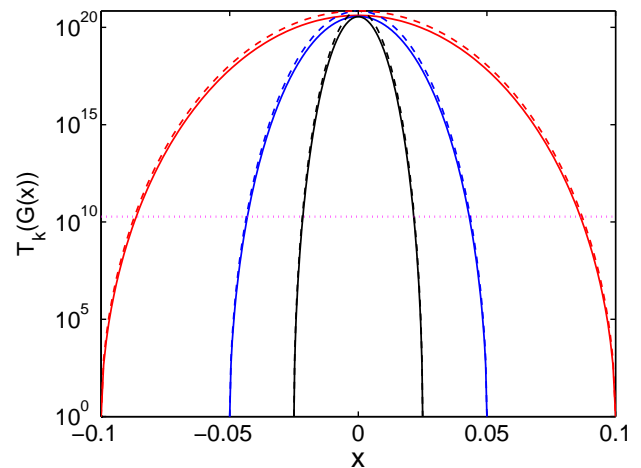


FIG. 2. (Color online.) The exp-semicircle filter for $k = 240$ and $a = 0.1$ (red lines), $k = 480$ and $a = 0.05$ (blue lines), $k = 960$ and $a = 0.025$ (black lines), with $ka = 24$. We have set $E_{\max} = 1$ and $E_{\min} = -1$. The solid lines are for the Chebyshev polynomial $T_k(F(x))$, where $F(x) = [2x^2 - (1 + a^2)] / (1 - a^2)$, while the dashed lines are for the approximation $y = \exp(2k\sqrt{a^2 - x^2}) \simeq T_k(F(x))$. The horizontal pink dotted line denotes the half maximum of the logarithm of filters. Note that $|T_k(F(x))| \leq 1$ when $x \notin [-a, a]$, thus the graphs of filter are restricted in $[-a, a]$.

$(-1)^k \cosh(k\Theta)$ for the lower end of the spectrum, where

$$\Theta = \cosh^{-1}\left(1 + \frac{2(a^2 - \mathcal{H}^2)}{E_{\max}^2 - a^2}\right). \quad (5)$$

Let $|\psi_{init}\rangle = \sum_i c_i |\phi_i\rangle + \sum_j d_j |\chi_j\rangle$ be a random initial state, with c_i and d_j the random coefficients, $|\phi_i\rangle$ the eigenstates inside \mathbb{L} , $|\chi_j\rangle$ the eigenstates outside \mathbb{L} . The filtration by $T_k(\mathcal{G})$ is

$$\begin{aligned} |\psi_{init}(k)\rangle &= T_k(\mathcal{F}) |\psi_{init}\rangle \\ &= \sum_i \left(e^{k\theta_1^i} + e^{-k\theta_1^i} \right) \frac{c_i}{2} |\phi_i\rangle + \sum_j \left(e^{ik\theta_2^j} + e^{-ik\theta_2^j} \right) \frac{d_j}{2} |\chi_j\rangle \\ &\simeq \frac{1}{2} \sum_i e^{k\theta_1^i} c_i |\phi_i\rangle, \end{aligned} \quad (6)$$

where $\theta_1^i = \cosh^{-1}\left(1 + 2(a^2 - E_i^2)/(E_{\max}^2 - a^2)\right)$, $\theta_2^j = \cos^{-1}\left(2(E_j^2 - a^2)/(E_{\max}^2 - a^2) - 1\right)$, E_i and E_j are eigenvalues corresponding to $|\phi_i\rangle$ and $|\chi_j\rangle$, respectively. In writing Eq. (6) we have ignored $(-1)^k$, as it does not affect the absolute value of coefficients and is a global phase at the end line. When a is tiny, i.e., $a^2 \ll E_{\max}^2$, one may further deduce $\theta_1^i \simeq 2\sqrt{a^2 - E_i^2}/E_{\max}$ via Taylor's expansion of $\cosh^{-1}(1+\epsilon)$, where ϵ is a small positive number. We thus obtain the exp-semicircle filter

$$T_k(\mathcal{F}) \simeq e^{\frac{2k}{E_{\max}} \sqrt{a^2 - \mathcal{H}^2}} \quad (7)$$

that peaked at $E_i = 0$, for eigenstates satisfying $-a \leq E_i \leq a$. In Fig. 2 the shape of Eq. 7 is also presented in dashed lines, which fits pretty well with the exact form.

With the initial conditions $T_0(\mathcal{F}) = 1$ and $T_1(\mathcal{F}) = \mathcal{F}$, the k th order Chebyshev polynomial can be efficiently determined using the recurrence relation Eq. (3). In this paper, we set the cut-off order $K = 18E_{\max}/a$. Such a filter exponentially (the fastest rate among all polynomials) amplifies the components of eigenstates inside \mathbb{L} . After the normalization, it essentially dampens those outside \mathbb{L} , generating the target state $|\psi_f\rangle \equiv |\psi_{init}(K)\rangle$ localized at the central spectrum.

C. Chebyshev Evolution

Now that there is a state $|\psi_f\rangle$ confined in the small subspace \mathbb{L} , we then make use of the oscillation property of the Chebyshev polynomial to efficiently generate a set of linearly-independent states, as large as possible. To achieve this goal, it is necessary to limit $E_i \in [-1, 1]$ (corresponding to x), within which the Chebyshev polynomial behave as a cosine-like function. This region is contrast to the requirement of the exp-semicircle filter, thus we need a different transformation of \mathcal{H} . Below we describe the specific details for the second application of the Chebyshev polynomial.

The original Hamiltonian \mathcal{H} needs to be shifted by E'_c and be rescaled by E'_0 , where $E'_c = \frac{1}{2}(E_{\min} + E_{\max})$ and

$E'_0 = \frac{1}{2}(-E_{\min} + E_{\max})$. In a similar way to the Eq. (4), we define the operator $\mathcal{G} = (\mathcal{H} - E'_c)/E'_0$, which is definitely bounded by -1 and 1 . Assuming $E_{\min} = -E_{\max}$ again, which does not affect the conclusion, then

$$\mathcal{G} = \frac{\mathcal{H}}{E_{\max}}. \quad (8)$$

At the same time, the parameter a is rescaled to $\tilde{a} = a/E_{\max}$ as well.

It is interesting to explore the Chebyshev evolution, i.e., the evolution governed by the operator $T_k(\mathcal{G})$ as k plays the role of time t . We now view the state generated in the Eq. (6) as the initial state, $|\psi_f\rangle = |\psi_{init}(K)\rangle = \alpha \sum_i c'_i |\phi_i\rangle$, where $c'_i = c_i e^{K\theta_1^i}$ and α is the normalization constant. Since $\|\mathcal{G}\| \leq 1$, we have $T_k(\mathcal{G}) = \cos(k\Omega)$, where

$$\Omega = \arccos(\mathcal{G}). \quad (9)$$

In this sense, the Chebyshev evolution is

$$\begin{aligned} |\psi_f(k)\rangle &= T_k(\mathcal{G}) |\psi_f\rangle \\ &= \frac{1}{2} \sum_j (e^{ik\omega_j} + e^{-ik\omega_j}) c'_j |\phi_j\rangle, \end{aligned} \quad (10)$$

where $\omega_j = \arccos(E_j/E_{\max})$. Certainly, this is not a physically legal time evolution, $T_k(\mathcal{G})$ is not even a unitary operator. Actually, it essentially represents a superposition of both forward and backward time propagation. Note that each time the polynomial order k is increased by 1, the evolution time is added by 1 as well. In this sense, the Chebyshev evolution is an extremely efficient (possibly the most one among all the polynomials) simulation of the quantum oscillations.

With the aid of the Chebyshev evolution, we are able to construct a near-orthonormal basis that spans the subspace \mathbb{L} . In detail, we want to collect a set of states as follows

$$\left\{ I, \sin\left(\frac{\pi\mathcal{G}}{\tilde{a}}\right), \dots, \sin\left(\frac{n\pi\mathcal{G}}{\tilde{a}}\right), \cos\left(\frac{\pi\mathcal{G}}{\tilde{a}}\right), \dots, \cos\left(\frac{n\pi\mathcal{G}}{\tilde{a}}\right) \right\} |\psi_f\rangle, \quad (11)$$

where n is an integer determined by the relation $2n + 1 \geq$ the dimension d of \mathbb{L} . More details can be found in Appendix. A. The k th order Chebyshev polynomial $T_k(\mathcal{G})$ can be similarly calculated as the last subsection. The cut-off order (evolution time) $K' = \lfloor n\pi/\tilde{a} \rfloor$. Note that according to the relations of discrete Fourier series, for a state $|\psi\rangle$ in \mathbb{L} that is uniformly distributed in the energy representation, we may have

$$\langle \psi | \sin\left(\frac{i\pi\mathcal{G}}{\tilde{a}}\right) \sin\left(\frac{j\pi\mathcal{G}}{\tilde{a}}\right) | \psi \rangle \simeq \delta_{ij}, \quad (12)$$

where positive integers $i, j \leq n$ and δ_{ij} is the Kronecker symbol. Such a relation holds between any two of the states in Eq. (11). However, we note the problem is that $|\psi_f\rangle$ is not the uniformly distributed state in Eq. (12).

This problem leads to the low precision of certain converged eigenvalues and the appearance of linearly dependent states. Therefore, the Eq. (11) is not expected to be an orthogonal basis, the number of states in it shall be d times a constant. We present the remained solution in the next subsection.

D. Subspace Diagonalization

Computing the basis $\{|\Psi_i\rangle : i = 1, \dots, 2n+1\}$ (Eq. (11)) by combination of the exp-semicircle filter and the Chebyshev evolution represents the most challenging aspect as well as the most time-consuming part of the method. Once the appropriate basis has been constructed, the task remained is more or less straightforward, i.e., to compute the eigenpairs of the projected Hamiltonian H . This is equivalent to solving the generalized eigenvalue problem:

$$HB = SBA. \quad (13)$$

Here, H and S denote the projected Hamiltonian and overlap matrices, respectively,

$$H_{ij} = \langle \Psi_i | \mathcal{H} | \Psi_j \rangle, S_{ij} = \langle \Psi_i | \Psi_j \rangle. \quad (14)$$

Λ is a diagonal matrix with the eigenvalues contained in $[-a, a]$ and the matrix B transforms the found basis Eq. (11) to the eigenstates $|\phi_j\rangle$ of \mathcal{H} ,

$$|\phi_j\rangle = \sum_{i=1}^{2n+1} B_{ij} |\Psi_i\rangle. \quad (15)$$

All these matrices are of size $(2n+1) \times (2n+1)$. Because of the small size of H , it can be stored in core memory. The necessary procedures are thus conveniently available in the LAPACK library [43].

Importantly, due to the special property of the Chebyshev polynomial, the computation of matrices H and S can even be achieved without an explicit computation and storage of the states $|\Psi_i\rangle$. This feature gives rise to a further improvement for the DACP method, both in computation time and memory consumption. On the other hand, for an overcomplete basis Eq. (11), the overlap matrix S is generally singular. We can use singular value decomposition to solve it. We show both the explicit expressions (denoted by $T_k(\mathcal{G})$ and $|\psi_f\rangle$ only) of matrices H and S , and the solution of the generalized eigenvalue problem in Appendix. B.

III. NUMERICAL RESULTS

We apply the method to the quantum spin-1/2 systems with two-body interactions. Such systems are good models for investigating a large class of important problems in quantum computing, solid state theory, and quantum

statistics [44–47]. A large amount of exact eigenvalues helps us to obtain the statistical properties, to distinguish quantum chaos from integrability, and serves as a benchmark to evaluate other approximate methods as well.

Generally speaking, the method can deal with the spin systems consists of couplings between any two of the N spins. Each of the Pauli matrix σ^α or the two coupling Pauli matrices $\sigma^\alpha \otimes \sigma^\beta$, where $\alpha, \beta = x, y, z$, is properly represented by a specific function.

We specify the spin model by two physical systems. One is the disordered one-dimensional transverse field Ising model [48], where the Hamiltonian is

$$H = \frac{1}{4} \sum_{i=1}^{N-1} J_{i,i+1} \sigma_i^x \sigma_{i+1}^x + \frac{1}{2} \sum_{i=1}^N \Gamma_i^z \sigma_i^z, \quad (16)$$

with σ_i the Pauli matrices for the spin i . This system is exactly solvable by Jordan-Wigner transformation [46], making it an ideal correctness checker for the DELDAV method. The nearest neighbor exchange interaction constants $J_{i,i+1}$ are random numbers that uniformly distributed in $[-J/\sqrt{N}, J/\sqrt{N}]$ with $J = 10$. The local random magnetic fields are represented by Γ_i^z , which are random numbers that uniformly distributed in the interval $[0, \Gamma]$ with $\Gamma = 1$.

Another system is the spin glass shards [13], which represents a class of global-range interacting systems that require relatively large bond dimensions to be tackled by the DMRG methods [49]. The Hamiltonian describing the system is

$$H = \sum_{i<j} J_{ij} \sigma_i^x \sigma_j^x + \sum_i \Gamma_i^z \sigma_i^z. \quad (17)$$

All symbols and parameters are the same as that of the above Ising model, except that the first summation runs over all possible spin pairs. This system is interesting because it presents two crossovers from integrability to quantum chaos and back to integrability again. In the limit $J/\Gamma \rightarrow 0$, the ground state is paramagnetic with all spins in the local field direction and the system is integrable [13]. In the opposite limit $J/\Gamma \rightarrow \infty$, the ground state is spin glass and the system is also integrable since there are N operators (σ_i^x) commuting with the Hamiltonian. A quantum chaos region exists between these two limits. $J = 10\Gamma$ is approximately the border from the quantum chaos to the integrable (the spin glass side) when $N = 20$ [13].

By employing the upper-bound-estimator, which costs little extra computation and bounds up the largest absolute eigenvalue E_0 , one may estimate $E_{\max} = E_0$ and $E_{\min} = -E_0$ [50]. For this setting we have utilized the symmetry of the density of states (DOS), a bell-shape profile centered at zero, in the many-spin systems. Since we want to find out 5,000 central eigenvalues, to span up the whole subspace \mathbb{L} we may set $n = 4,000$, corresponding to a dimension 8,001 if the states in Eq. (11) were

all linearly independent. The overlap matrix S is generally singular. The approximate distribution of DOS $\rho(E)$ may be efficiently calculated through the Fourier transformation of a time evolved wave function or through a better estimation method given in [51]. The parameter a is appropriately chosen to ensure that the number of eigenstates contained in $[-a, a]$ is around 7,000 (as illustrated in Fig. 3, the precision of some converged eigenvalues may be lower than required).

In practice, sometimes there is a batch of highly near-degenerate eigenvalues, with level spacings as small as $10^{-7}\Gamma$ while the average spacing is $10^{-5}\Gamma$. It is hard (two magnitudes longer time) for the Chebyshev evolution to discriminate such closely lied pair of eigenvalues. We thus employ the block filter technique, which means a block of states is filtered or evolved ‘simultaneously’, in programming of our method [41]. The idea is that two or several random states in the degenerate subspace are always linearly independent. For each numerical test, a block of 5 initial trial states is randomly generated and used while the parameter n is adjusted to $n = 800$ accordingly.

By these settings, we perform numerical tests on the above two systems to show the high exactness and efficiency of our method. All the timing information reported in this manuscript is obtained from calculations on the Intel(R) Xeon(R) CPU E7-8880 v4, using sequential mode.

In Fig. 3 we present the relative error η in logarithmic scale versus the system energy E_{exact} , for the Ising model with $N = 19$ and the spin glass shards with $N = 17$. We define the relative error η of the computed central eigenvalues E as

$$\eta = \left| \frac{E - E_{\text{exact}}}{E_{\text{exact}}} \right|.$$

Exact eigenvalues of both systems have been obtained by other reliable methods. For the Ising model, we make use of the famous Jordan-Wigner transformation to reduce the original $2^N \times 2^N$ matrix to a $2N \times 2N$ one, and restore the full spectrum of the original Hamiltonian [46]. For the spin glass shards we simply utilize the function *eigs* of MATLAB, to find 5,000 eigenvalues closest to $E = 0$. As for our numerical tests, the parameter a in Fig. 3 is 0.036Γ and 0.16Γ for (a) and (b), respectively. In computing the Ising model, the number of eigenvalues satisfying $\eta < 10^{-6}$ is not enough (less than 5,000) by the settings mentioned above. By changing the block size to 10 and the parameter n to 500, we then collect enough eigenvalues. The number of eigenvalues satisfying the condition is 5,385 for (a) and 5,000 (all the exact eigenvalues we have) for (b). We note that the total number of converged eigenvalues is 6,232 and 5,910, respectively.

The spike around $E = 0$ for both figures is due to the smallness of the denominator E_{exact} . The smallest absolute eigenvalue is about $4.4 \times 10^{-6}\Gamma$ for (a) and $2.9 \times 10^{-5}\Gamma$ for (b). Besides, there is a flat plateau in the middle of the figures. In fact, it indicates that for those

eigenvalues around $E = 0$ we encounter the numerical error, i.e., the absolute error reaches the limit of the double precision representation. In Fig. 3 (a) one may observe other spikes, which does not appear in (b). Each of those spikes corresponds to a cluster of eigenvalues lying extremely close to each other. The integrability of the Ising model implies the absence of level repulsion and a Poissonian distribution of energy level spacings. We speculate that the Chebyshev evolution does not function well for closely lied eigenvalues, as they give quite similar phase contributions to the final states. To significantly amplify the phase difference $\exp(i\Delta Et)$ it requires $t \simeq 1/\Delta E$, where ΔE is the energy difference. The solution is to increase the block size to match up with the dimension of near-degenerate subspace. Ignoring the central plateau and the spikes, the distribution of η fits fairly well to the

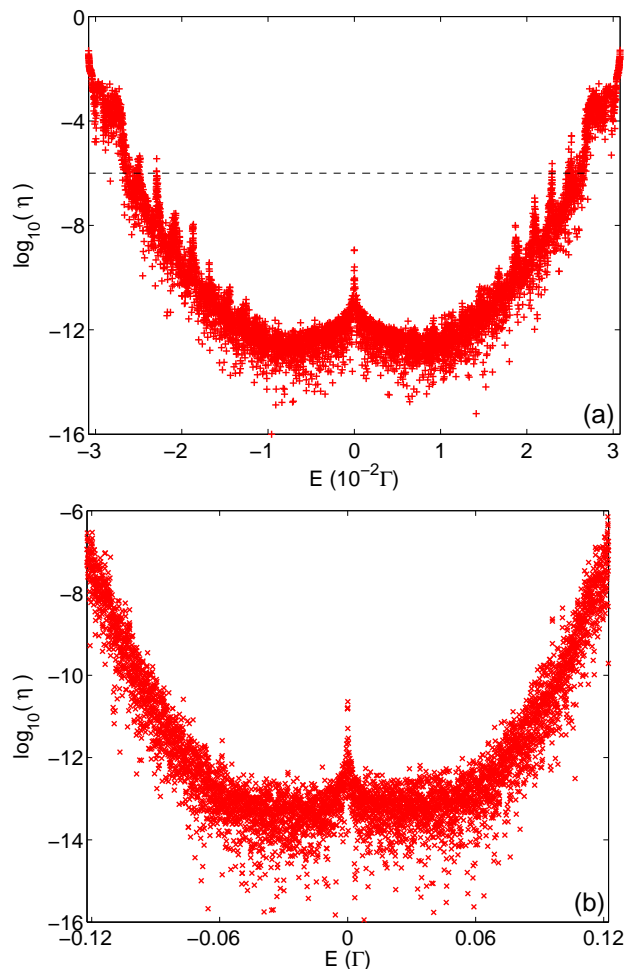


FIG. 3. (Color online.) The relative error $\eta = |(E - E_{\text{exact}})/E_{\text{exact}}|$ in logarithmic scale of the calculated eigenvalues, is shown for (a) Ising model with $N = 19$ and (b) spin glass shards model with $N = 17$. The x -axis is the system energy measured by (a) $10^{-2}\Gamma$ and (b) Γ . The number of eigenvalues satisfying $\eta < 10^{-6}$ (black dashed line) is 5,385 for (a) and 5,000 for (b). Both figures fit well with the shape of exp-semicircle filter in Fig. 2.

shape of the corresponding exp-semicircle filter.

In Fig. 4 we compare the computation time T (CPU time in seconds) of our method with that of the shift-invert method. Each of the numerical tests finds around 5,000 eigenvalues for either of the two spin systems. For our method, we have discarded the time consumed by the subspace diagonalization, as it is a constant time and does not affect the scaling behavior. This subspace diagonalization time is roughly 700 CPU seconds in each test. Such a constant is completely negligible for $N \geq 17$ systems.

The shift-invert method is implemented by the *eigs* function of Matlab R2019b, which employs the implicitly restarted Arnoldi method (ARPACK) [52]. It is widely used in computing eigenpairs at the middle of the spectrum for quantum spin systems, to name a few, like in [8, 30–32]. However, the matrix size of \mathcal{H}^{-1} (inverse of the Hamiltonian) grows rather fast as the system size N increases (proportional to 4^N), demanding a large amount of memory. For example, in our tests it consumes 573 GB of memory for $N = 17$ systems. On the contrary, the DACP method works in a matrix-vector product mode that does not need an explicit matrix representation, its memory requirements depend only on the dimension of the subspace. By the above settings it occupies around 5.6 GB of memory for $N \leq 20$ systems.

As shown in Fig. 4, the scaling among these two methods is comparable. To compare quantitatively, we extract the scaling constants α of the four lines by fitting the numerical results, where α is defined by $T = T_0 \exp(\alpha N)$.

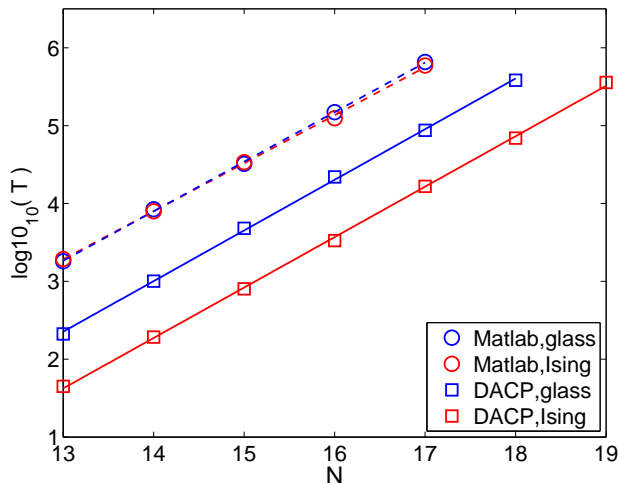


FIG. 4. (Color online.) Scaling behavior measured by the computation time T (CPU seconds) in logarithmic scale, versus the system size N , with the DACP method (solid lines with squares) compared to the shift-invert method (dashed lines with circles) for the Ising model (red) and the spin glass shards (blue). Each of the numerical tests, represented either by squares or circles, finds 5,000 central eigenvalues. All the four lines are obtained via linear fitting. Evidently, the DACP method converges faster.

TABLE I. Scaling constants α by linear fitting of the four curves in Fig. 4.

α	DACP method	Shift-invert method
Ising	1.49	1.42
Glass	1.50	1.47

The values of α are shown in Table I. Indeed, the four scaling constants are quite close, with a little worse for the DACP method. Whereas, it is about 30 times faster than the shift-invert method for the Ising model and 8 times faster for the spin glass shards. Suppose that α are constants, then the DACP method's advantage in time cost keeps on until $N \geq 60$ systems, which is a condition far beyond the memory capacity. Also, as illustrated by the numerical tests in [8], the factorization for finding \mathcal{H}^{-1} takes an increasing time compared to the other computation steps. Considering the factorization part only, the execution time in [8] exhibits a scaling constant $\alpha \simeq 1.66$, indicating a worse scaling behavior for large systems. The efficiency of our method is thus confirmed.

Moreover, as the shift-invert method essentially finds the ground energy of \mathcal{H}^{-1} , which is usually not a sparse matrix, its computation time T is not affected by the sparsity of the Hamiltonian and the two dashed lines nearly coincide. On the other hand, the DACP method employs the polynomial combination of \mathcal{H} acting on the states, its computation time T is heavily influenced by the number of Pauli operators of the specific Hamiltonian. For example, when $N = 18$ the computation time

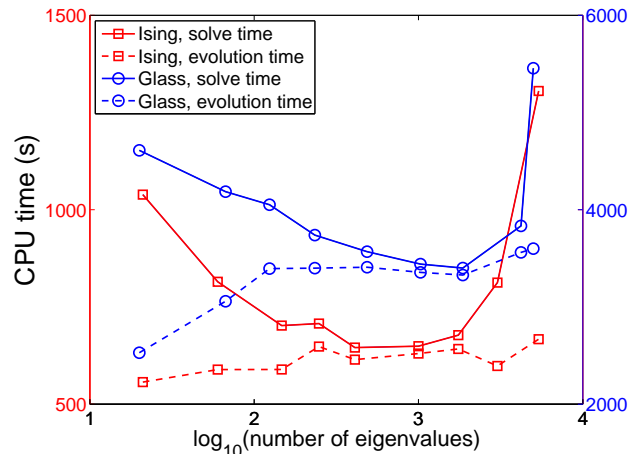


FIG. 5. (Color online.) Computation time required versus number of converged eigenvalues, for the Ising model (red lines with squares, left y-axis) and the spin glass shards (blue lines with circles, right y-axis), using the DACP method. Both systems are of size $N = 15$. The solid lines show the full solve time, including the exp-semicircle filtration, Chebyshev evolution and subspace diagonalization. The dashed lines represent the execution time for the Chebyshev evolution only. Obviously, it is lowly correlated with the number of converged eigenvalues.

T for the spin glass shards is 5.5 times to that for the Ising model, while the number of Pauli operators is 6.2 times. Considering this effect, our method is still advantageous over the shift-invert approach in the worst case where the exchange interactions run over all possible spin pairs and all three dimensions.

In Fig. 5 we show the time required for the computation versus number of eigenvalues, for the two systems of size $N = 15$. The x-axis represents the number of converged eigenvalues that satisfying the condition $\eta(E) \leq 10^{-6}$ in each test. Changing the parameter a adjusts the dimension of the target subspace, which corresponds to the number of eigenvalues requested. For a specific system, a smaller value of a means fewer eigenvalues are requested. Assuming the DOS is constant in the interval $[-a, a]$, the parameter a is proportional to the number of eigenvalues.

Note that the dashed lines show the computation time required for the Chebyshev evolution. It is easily seen that the dashed lines show a low correlation with the parameter a , to be discussed in Sec. IV. The small vibrations of the dashed lines may due to the changes of average DOS as a is varied. Recall that we have divided the DACP method as three parts: exp-semicircle filtration, Chebyshev evolution, and subspace diagonalization. Their computation times are denoted as t_f , t_c , and t_d , respectively. For the left end of the figure, the exp-semicircle filtration dominates the full computation time, since $t_f \propto 36E_{\max}/a$ is inversely proportional to the parameter a . On the other hand, the time cost for the subspace diagonalization is proportional to the cube of its dimension, or to the cube of the parameter a . Thus, t_d dominates the full computation time at the right end of the figure. In between the Chebyshev evolution constitutes the part of major time cost, where $t_c \propto [n\pi E_{\max}/a]$. For systems with larger spins, this region is broadened, as the matrix-vector product time is longer, while t_d is invariant unless the required number of eigenvalues is changed.

IV. DISCUSSION AND CONCLUSION

Although using the Chebyshev polynomial in common, there is a feature distinguishes our method from those polynomial filtering ones, which explore the combination of Chebyshev filter with Krylov projection methods [21, 37, 40, 41, 53]. Firstly note that when counting the actions of the Hamiltonian \mathcal{H} , the time cost for the exp-semicircle filter and the Chebyshev evolution is $t_f \propto 36E_{\max}/a$ and $t_c \propto [n\pi E_{\max}/a]$, respectively. Therefore, in finding thousands of eigenvalues, the Chebyshev evolution costs the major part of time (about two magnitudes longer compared to the filtration). Since the DOS $\rho(E)$ is usually a bell-shape profile centered at zero in spin systems, and typically a is a tiny parameter ($a/E_{\max} \simeq 1/200$ for $N = 19$), one may view $\rho(E)$ as a constant parameter $\bar{\rho}$ in $[-a, a]$. Recall the number of

eigenvalues contained in this interval is about $2n + 1$,

$$\bar{\rho} \simeq \frac{2n + 1}{2a} \simeq \frac{n}{a}. \quad (18)$$

The time consumption $t_c \propto [\bar{\rho}\pi E_{\max}]$ is thus related only to the average DOS, not to the number of eigenvalues. As is confirmed in Fig. 5, the performance of DACP method is approximately the same between finding 20 and 5,000 eigenvalues. The difference of time consumption mainly comes from the hardness to fully diagonalize the subspace representation of \mathcal{H} . Such a feature may bring a belief that we have achieved an optimal solution. It is contrast to those filtering methods, which always require a larger amount of filtration and reorthogonalization, thus a longer convergence time, in finding more eigenvalues. In fact, as illustrated in [8], we may conclude that the computation time is roughly proportional to the number of eigenvalues required for the iterative methods. The DACP method is thus desirable for computing a large amount of eigenvalues.

Seeking statistical properties of eigenvalues is a hard problem and exact numerical diagonalization is an important tool for its investigation. In conclusion, we propose the dual application of Chebyshev polynomial method to find out thousands of central eigenvalues with high precision. The DACP method is applicable to any sparse matrices, but in this manuscript we focus on the specific details to apply it to quantum many-spin systems. We have explored the excellent properties of Chebyshev polynomial to efficiently filter out those non-central part of spectrum and to construct the appropriate subspace. Both processes may have achieved the highest efficiency among all polynomials.

The numerical tests for the Ising model and the spin glass shards confirm the exactness and efficiency of the DACP method. Compared to the widely used shift-invert method, DACP gives a considerable increase in the speed of computations, for the Ising model up to a factor of 30 while for the spin glass shards the increase in speed is less but still considerable (a factor of 8). The DACP method is more advantageous when the number of interaction terms is not too large. At the same time, it also gives a drastic decrease in memory requirement, up to a factor of 100 for $N = 17$ spin systems and even more for larger spins. These conclusions hold for any types of spin systems.

Appendix A: detailed deductions

Here we derive explicit expressions showing how to construct the set Eq. (11) via the Chebyshev evolution. We focus on the case that $a \ll E_{\max}$, which is fairly reason-

able for large ($N \geq 15$) spin systems.

$$\begin{aligned}
|\psi_f(k)\rangle &= T_k(\mathcal{G})|\psi_f\rangle \\
&= \sum_j \cos(k\omega_j) c'_j |\phi_j\rangle \\
&\simeq \sum_j \cos\left(\frac{k\pi}{2} - \frac{kE_j}{E_{\max}}\right) c'_j |\phi_j\rangle \\
&= \begin{cases} (-1)^n \sum_j \cos\left(k\frac{E_j}{E_{\max}}\right) c'_j |\phi_j\rangle, & k = 2n \\ (-1)^n \sum_j \sin\left(k\frac{E_j}{E_{\max}}\right) c'_j |\phi_j\rangle, & k = 2n + 1. \end{cases} \quad (\text{A1})
\end{aligned}$$

Using the fact that when x is small, $\arccos(x) = \pi/2 - x + o(x)$, we have $\omega_j = \arccos(E_j/E_{\max}) \simeq \pi/2 - E_j/E_{\max}$ at the third line of Eq. (A1). Therefore, we have the expression

$$T_k(\mathcal{G}) \simeq \begin{cases} (-1)^n \cos(k\mathcal{G}), & k = 2n \\ (-1)^n \sin(k\mathcal{G}), & k = 2n + 1. \end{cases} \quad (\text{A2})$$

We then conduct a Chebyshev evolution with a cut-off order $K' = \lfloor n\pi/\tilde{a} \rfloor$, record both $T_{k-1}(\mathcal{G})|\psi_f\rangle$ and $T_k(\mathcal{G})|\psi_f\rangle$ when $k = \lfloor m\pi/\tilde{a} \rfloor$, where $m = 1, \dots, n$. After the evolution is done, the set of states Eq. (11) is automatically generated.

Appendix B: evaluation of matrix elements and solution of the generalized eigenvalue problem

As shown in Appendix. A, we may rewrite the basis $\{|\Psi_i\rangle : i = 1, \dots, 2n + 1\}$ using the Chebyshev polynomials:

$$\{I, T_{k_1-1}(\mathcal{G}), T_{k_1}(\mathcal{G}), \dots, T_{k_n-1}(\mathcal{G}), T_{k_n}(\mathcal{G})\} |\psi_f\rangle, \quad (\text{B1})$$

where $k_m = \lfloor m\pi/\tilde{a} \rfloor$, $m = 1, \dots, n$, with $|\Psi_1\rangle = |\psi_f\rangle$, $|\Psi_2\rangle = T_{k_1-1}(\mathcal{G})|\psi_f\rangle$, $|\Psi_3\rangle = T_{k_1}(\mathcal{G})|\psi_f\rangle$, etc.

The element $S_{ij} = \langle \Psi_i | \Psi_j \rangle = \langle \psi_f | T_x(\mathcal{G}) T_y(\mathcal{G}) | \psi_f \rangle$, where x and y are directly determined by i and j . The correspondence is one to one. By making use of the relation

$$T_i(\mathcal{H}) T_j(\mathcal{H}) = \frac{1}{2} (T_{i+j}(\mathcal{H}) + T_{|i-j|}(\mathcal{H})), \quad (\text{B2})$$

we may find the matrix element without recording the states during the Chebyshev evolution. Instead, we simply record the values $\langle \psi_f | T_k(\mathcal{G}) | \psi_f \rangle$ and $\langle \psi_f | \mathcal{H} T_k(\mathcal{G}) | \psi_f \rangle$ at an appropriate time, i.e., when $k = \lfloor m\pi/\tilde{a} \rfloor - 1$ and $k = \lfloor m\pi/\tilde{a} \rfloor$.

Finally, we arrive at the explicit expressions of matrix

elements

$$S_{ij} = \frac{1}{2} \langle \psi_f | (T_{x+y}(\mathcal{G}) + T_{|x-y|}(\mathcal{G})) | \psi_f \rangle, \quad (\text{B3})$$

$$H_{ij} = \frac{1}{2} \langle \psi_f | \mathcal{H} (T_{x+y}(\mathcal{G}) + T_{|x-y|}(\mathcal{G})) | \psi_f \rangle. \quad (\text{B4})$$

For the generalized eigenvalue problem Eq. (13), the Hermitian matrix S is first diagonalized as

$$S = V \Lambda_s V^\dagger, \quad (\text{B5})$$

where V is the eigenvector matrix for S , $VV^\dagger = I$, and Λ_s is the associated eigenvalue matrix. Since S is generally singular, we then contract the $(2n+1) \times (2n+1)$ matrix V by elimination of the columns associated with eigenvalues with absolute value below a cutoff $\epsilon = 10^{-12}$. Denoting the number of retained eigenvalues as m , the contracted eigenvector matrix \tilde{V} is of order $(2n+1) \times m$, and

$$\tilde{S} = \tilde{V} \tilde{\Lambda}_s \tilde{V}^\dagger. \quad (\text{B6})$$

The next step is to form the contracted Hamiltonian matrix \tilde{H} . Since

$$I = \left(\tilde{\Lambda}_s^{-\frac{1}{2}} \tilde{V}^\dagger \right) \tilde{S} \left(\tilde{V} \tilde{\Lambda}_s^{-\frac{1}{2}} \right), \quad (\text{B7})$$

denoting the transformation matrix $U = \tilde{V} \tilde{\Lambda}_s^{-\frac{1}{2}}$, the contracted $m \times m$ Hamiltonian matrix is

$$\tilde{H} = U^\dagger H U. \quad (\text{B8})$$

The Hermitian matrix \tilde{H} of order $m \times m$ with m around 10^3 to 10^4 is then diagonalized directly

$$\tilde{H} = \tilde{Y} \tilde{\Lambda} \tilde{Y}^\dagger, \quad (\text{B9})$$

where \tilde{Y} is the eigenvector matrix of \tilde{H} and $\tilde{\Lambda}$ is a diagonal matrix with desired eigenvalue approximations of the original Hamiltonian \mathcal{H} contained in $[-a, a]$. The eigenstates of the projected Hamiltonian H may be obtained through elementary matrix algebra:

$$B = U \tilde{Y} = \tilde{V} \tilde{\Lambda}_s^{-\frac{1}{2}} \tilde{Y}. \quad (\text{B10})$$

Denoting the Eq. (B1) as a $2^N \times (2n+1)$ matrix A with $|\chi_i\rangle$ being the i -th column, the eigenstate approximations of the original Hamiltonian \mathcal{H} contained in $[-a, a]$ is

$$\Phi = AB = A \tilde{V} \tilde{\Lambda}_s^{-\frac{1}{2}} \tilde{Y}. \quad (\text{B11})$$

We finally get the answers $\tilde{\Lambda}$ and Φ .

ACKNOWLEDGMENT

We thank X.-H. Deng for discussions. This work is supported by the NSFC Grant No. 91836101, No. 11574239, and No. U1930201. The numerical calculations in this paper have been done on the supercomputing system in the Supercomputing Center of Wuhan University.

-
- [1] F. Haake, *Quantum Signatures of Chaos* (Springer-Verlag, Berlin Heidelberg, 2010).
- [2] T. A. Brody, J. Flores, J. B. French, P. A. Mello, A. Pandey, and S. S. M. Wong, Random-matrix physics: spectrum and strength fluctuations, *Rev. Mod. Phys.* **53**, 385 (1981).
- [3] O. Bohigas, M. J. Giannoni, and C. Schmit, Characterization of chaotic quantum spectra and universality of level fluctuation laws, *Phys. Rev. Lett.* **52**, 1 (1984).
- [4] M. L. Mehta, *Random Matrices* (Academic Press, New York, 1991).
- [5] A. Relaño, J. M. G. Gómez, R. A. Molina, J. Retamosa, and E. Faleiro, Quantum chaos and $1/f$ noise, *Phys. Rev. Lett.* **89**, 244102 (2002).
- [6] D. Basko, I. Aleiner, and B. Altshuler, Metal-insulator transition in a weakly interacting many-electron system with localized single-particle states, *Ann. Phys.* **321**, 1126 (2006).
- [7] R. Nandkishore and D. A. Huse, Many-body localization and thermalization in quantum statistical mechanics, *Annu. Rev. Condens. Matter Phys.* **6**, 15 (2015).
- [8] F. Pietracaprina, N. Macé, D. J. Luitz, and F. Alet, Shift-invert diagonalization of large many-body localizing spin chains, *SciPost Phys.* **5**, 45 (2018).
- [9] V. Khemani, F. Pollmann, and S. L. Sondhi, Obtaining highly excited eigenstates of many-body localized hamiltonians by the density matrix renormalization group approach, *Phys. Rev. Lett.* **116**, 247204 (2016).
- [10] D. Pekker, G. Refael, E. Altman, E. Demler, and V. Oganesyan, Hilbert-glass transition: New universality of temperature-tuned many-body dynamical quantum criticality, *Phys. Rev. X* **4**, 011052 (2014).
- [11] F. Alet and N. Laflorencie, Many-body localization: An introduction and selected topics, *C. R. Phys.* **19**, 498 (2018).
- [12] B. I. Shklovskii, B. Shapiro, B. R. Sears, P. Lambrianides, and H. B. Shore, Statistics of spectra of disordered systems near the metal-insulator transition, *Phys. Rev. B* **47**, 11487 (1993).
- [13] B. Georgeot and D. L. Shepelyansky, Integrability and quantum chaos in spin glass shards, *Phys. Rev. Lett.* **81**, 5129 (1998).
- [14] R. Blankenbecler and R. L. Sugar, Projector monte carlo method, *Phys. Rev. D* **27**, 1304 (1983).
- [15] A. W. Sandvik and J. Kurkijärvi, Quantum monte carlo simulation method for spin systems, *Phys. Rev. B* **43**, 5950 (1991).
- [16] S. R. White, Density matrix formulation for quantum renormalization groups, *Phys. Rev. Lett.* **69**, 2863 (1992).
- [17] G. Vidal, Efficient simulation of one-dimensional quantum many-body systems, *Phys. Rev. Lett.* **93**, 040502 (2004).
- [18] G. Vidal, Entanglement renormalization, *Phys. Rev. Lett.* **99**, 220405 (2007).
- [19] F. Verstraete, V. Murg, and J. Cirac, Matrix product states, projected entangled pair states, and variational renormalization group methods for quantum spin systems, *Adv. Phys.* **57**, 143 (2008).
- [20] T. Ericsson and A. Ruhe, The spectral transformation lanczos method for the numerical solution of large sparse generalized symmetric eigenvalue problems, *Math. Comput.* **35**, 1251 (1980).
- [21] R. E. Wyatt, Matrix spectroscopy: Computation of interior eigenstates of large matrices using layered iteration, *Phys. Rev. E* **51**, 3643 (1995).
- [22] T. J. Minehardt, J. D. Adcock, and R. E. Wyatt, Enhanced matrix spectroscopy: The preconditioned green-function block lanczos algorithm, *Phys. Rev. E* **56**, 4837 (1997).
- [23] E. Y. Loh, J. E. Gubernatis, R. T. Scalettar, S. R. White, D. J. Scalapino, and R. L. Sugar, Sign problem in the numerical simulation of many-electron systems, *Phys. Rev. B* **41**, 9301 (1990).
- [24] M. Troyer and U.-J. Wiese, Computational complexity and fundamental limitations to fermionic quantum monte carlo simulations, *Phys. Rev. Lett.* **94**, 170201 (2005).
- [25] R. Orús, A practical introduction to tensor networks: Matrix product states and projected entangled pair states, *Ann. Phys.* **349**, 117 (2014).
- [26] J. Eisert, M. Cramer, and M. B. Plenio, Colloquium: Area laws for the entanglement entropy, *Rev. Mod. Phys.* **82**, 277 (2010).
- [27] C. Lanczos, An iteration method for the solution of the eigenvalue problem of linear differential and intergral operators, *J. Res. Natl. Bur. Stand.* **45**, 255 (1950).
- [28] V. A. Mandelsham and H. S. Taylor, A simple recursion polynomial expansion of the green's function with absorbing boundary conditions. application to the reactive scattering, *J. Chem. Phys.* **103**, 2903 (1995).
- [29] Z. Bai, J. Demmel, J. Dongarra, A. Ruhe, and H. van der Vorst (Eds.), *Templates for the Solution of Algebraic Eigenvalue Problems: A Practical Guide*. (SIAM, Philadelphia, 2000).
- [30] D. J. Luitz, N. Laflorencie, and F. Alet, Many-body localization edge in the random-field heisenberg chain, *Phys. Rev. B* **91**, 081103 (2015).
- [31] P. Sierant and J. Zakrzewski, Model of level statistics for disordered interacting quantum many-body systems, *Phys. Rev. B* **101**, 104201 (2020).
- [32] M. Hopjan and F. Heidrich-Meisner, Many-body localization from a one-particle perspective in the disordered one-dimensional bose-hubbard model, *Phys. Rev. A* **101**, 063617 (2020).
- [33] J. Šuntajs, J. Bonča, T. c. v. Prosen, and L. Vidmar, Ergodicity breaking transition in finite disordered spin chains, *Phys. Rev. B* **102**, 064207 (2020).
- [34] R. Li, Y. Xi, E. Vecharynski, C. Yang, and Y. Saad, A thick-restart lanczos algorithm with polynomial filtering for hermitian eigenvalue problems, *SIAM J. Sci. Comput.* **38**, A2512 (2016).
- [35] P. Sierant, M. Lewenstein, and J. Zakrzewski, Polynomially filtered exact diagonalization approach to many-body localization, *Phys. Rev. Lett.* **125**, 156601 (2020).
- [36] H. Guan and W. Zhang, Delta-davidson method for interior eigenproblem in many-spin systems (2020), arXiv:2011.01554.
- [37] A. Pieper, M. Kreutzer, A. Alvermann, M. Galgon, H. Fehske, G. Hager, B. Lang, and G. Wellein, High-performance implementation of chebyshev filter diagonalization for interior eigenvalue computations, *J. Comput. Phys.* **325**, 226 (2016).

- [38] J. C. Mason and D. C. Handscomb, *Chebyshev Polynomials* (CRC Press LLC, Boca Raton, 2003).
- [39] T. J. Rivlin, *An Introduction to the Approximation of Functions* (Blaisdell Pub. Co, Waltham, 1969).
- [40] Y. Zhou and Y. Saad, A chebyshev-davidson algorithm for large symmetric eigenproblems, *SIAM J. Matrix Anal. Appl.* **29**, 954 (2007).
- [41] Y. Zhou, A block chebyshev-davidson method with inner-outer restart for large eigenvalue problems, *J. Comput. Phys.* **229**, 9188 (2010).
- [42] D. Poulin and P. Wocjan, Preparing ground states of quantum many-body systems on a quantum computer, *Phys. Rev. Lett.* **102**, 130503 (2009).
- [43] E. Anderson, Z. Bai, C. Bischof, J. Demmel, J. Dongarra, J. D. Cruz, A. Greenbaum, S. Hammarling, A. McKenney, S. Ostrouchov, and D. Sorensen, *LAPLACK User's Guide—Release 2.0* (Society for Industrial and Applied Mathematics, Philadelphia, 1994).
- [44] M. A. Nielsen and I. L. Chuang, *Quantum Computation and Quantum Information* (Cambridge University Press, Cambridge, England, 2011).
- [45] N. N. Bogolubov and J. N. N. Bogolubov, *Introduction to Quantum Statistical Mechanics* (World Scientific Publishing Co Pte Ltd, Singapore, 2009).
- [46] S. Sachdev, *Quantum Phase Transitions* (Cambridge University Press, Cambridge, England, 2011).
- [47] A. Dutta, G. Aeppli, B. K. Chakrabarti, U. Divakaran, T. F. Rosenbaum, and Diptiman Sen, *Quantum Phase Transitions in Transverse Field Spin Models: From Statistical Physics to Quantum Information* (Cambridge University Press, Cambridge, England, 2015).
- [48] D. S. Fisher, Critical behavior of random transverse-field ising spin chains, *Phys. Rev. B* **51**, 6411 (1995).
- [49] U. Schollwöck, The density-matrix renormalization group, *Rev. Mod. Phys.* **77**, 259 (2005).
- [50] Y. Zhou and R.-C. Li, Bounding the spectrum of large hermitian matrices, *Linear Algebra Appl.* **435**, 480 (2011).
- [51] A. Hams and H. De Raedt, Fast algorithm for finding the eigenvalue distribution of very large matrices, *Phys. Rev. E* **62**, 4365 (2000).
- [52] R. B. Lehoucq, D. C. Sorensen, and C. Yang, *ARPACK User's Guide: Solution of Large Scale Eigenvalue Problems with Implicitly Restarted Arnoldi Methods* (SIAM, Philadelphia, 1998).
- [53] H. R. Fang and Y. Saad, A filtered lanczos procedure for extreme and interior eigenvalue problems, *SIAM J. Sci. Comput.* **34**, A2220 (2012).